Graphene and graphene nanoribbons on InAs(110) and Au/InAs(110) surfaces: An *ab initio* study

D. P. Andrade and R. H. Miwa
Instituto de Física, Universidade Federal de Uberlândia Caixa Postal 593, 38400-902, Uberlândia, Minas Gerais, Brazil

G. P. Srivastava
School of Physics, University of Exeter, Stocker Road, Exeter EX4 4QL, United Kingdom
(Received 4 June 2011; revised manuscript received 13 August 2011; published 21 October 2011)

We have performed an *ab initio* investigation of graphene adsorption on clean and Au-covered InAs(110) surfaces. Total energy results reveal that the graphene sheet is weakly attached to such surfaces, with adsorption energy of approximately 25 meV/(C atom). Graphene nanoribbons, on the other hand, are more strongly adsorbed, with adsorption energy of approximately 45 meV/(C atom). Based upon our electronic band structure calculations, we find that there are small net charge transfers between the graphene sheet or ribbon and the clean or Au-covered InAs(110) surface. There is an electronic charge displacement in the graphene-surface interface region, giving rise to an electric dipole moment along the surface normal. Scanning tunneling microscopy simulations lend support to the recently proposed "transparency" effect of the graphene sheet adsorbed on the clean InAs(110) surface [He *et al.*, Nano Lett. **10**, 3446 (2010)] and suggest that the effect is maintained for adsorption on the metallic Au/InAs(110) surface.

DOI: 10.1103/PhysRevB.84.165322 PACS number(s): 71.15.Nc, 71.15.Mb, 73.20.At

I. INTRODUCTION

Among the currently synthesized carbon nanostructures, carbon nanotubes[1] and graphene sheets[2] possess remarkable electronic, structural, and mechanical properties and are considered promising for several applications, addressing the development of new (nano)devices. For instance, carbon nanotubes (CNTs) present one-dimensional electronic confinement along the growth direction, with metallic or semiconductor electronic character depending on their helicity and diameter. Similarly, stripes of graphene a few nanometers wide, the so-called graphene nanoribbons (GNRs), also exhibit one-dimensional electronic confinement (along the ribbon growth direction), with their electronic properties depending on the atomic structure of the ribbon edge sites.[3–5] In contrast, an isolated graphene sheet is a zero-gap semiconductor material, with its electronic states characterized by two-dimensional confinement, a linear energy-momentum dispersion, and a very high electronic mobility of around 200000 cm^2/V s.[6] Many current material science investigations are focused on studies of fundamental graphene physics[7] as well as addressing technological applications, such as high-frequency transistors.[8]

The electronic and structural properties of carbon nanostructures may change upon their interaction with solid surfaces. Indeed, there is a strong reduction in the electron mobility for graphene deposited on a silicon dioxide (SiO_2) substrate.[9] Soares *et al.*[10] have examined the modulation of the electronic properties of CNTs adsorbed on α-quartz surfaces. Theoretical and experimental studies have proposed that the electronic properties of CNTs, adsorbed on hydrogen-passivated Si(001) surfaces, can be tuned by modifying the surface stoichiometry[11–15] as well as the silicon surface geometry.[16] Further theoretical studies have examined the electronic and magnetic properties of GNRs attached to Si(001) surfaces.[17] Experimental investigations[18] have verified a noncovalent doping of CNTs adsorbed on III-V (110) surfaces. Such noncovalent doping has also been verified for graphene adsorbed on SiO_2, though the results are controversial.[19–21] As for the CNT/III-V(110) semiconductor systems, there are experimental works addressing the electronic and structural properties of graphene/GaAs(110) and graphene/InAs(110) systems.[22] The authors of Ref. 22 examined the "transparency" property of graphene sheets deposited on these surfaces from an analysis of scanning tunneling microscopy (STM) images. Their findings were supported by *ab initio* calculations. In contrast to CNT/III-V(110) systems, experimental investigations do not find any evidence of doping processes for graphene/III-V(110) systems.[18] However, first-principles calculations suggest that graphene can be doped if it is deposited on *n*- or *p*-type doped III-V(110) substrates.[23] In a comprehensive theoretical work, Khomyakov *et al.*[24] studied the electronic charge transfer for graphene sheets adsorbed on metal surfaces. They examined both graphene physisorbed systems [e.g., graphene on Au(111)] as well as chemisorbed systems [e.g., graphene on Ni(111)] and reported *p*-type doping for graphene on Au(111).

Based upon the recent investigations on graphene adsorbed on solid surfaces, we can infer that graphene on metal-covered semiconductor surfaces represents a new and interesting system to be considered for the development of electronic devices. In this paper, we present an *ab initio* total energy study of a graphene sheet and a graphene nanoribbon adsorbed on the clean and submonolayer Au-metal-covered (110) surfaces of the semiconductor InAs. We find that the graphene adsorption process is ruled by the van der Waals (vdW) interaction with the surface. For the graphene sheet we find adsorption energies in the range 20–30 meV/(C atom). Due to the presence of edges, the adsorption energy of the GNR increases by ~4.5 meV/C for the Au-covered InAs(110) surface. The transparency effect of the graphene sheet has been examined through STM simulations. The electronic properties of graphene are weakly perturbed, but there is the formation of an electronic dipole at the graphene-surface interface.

II. COMPUTATIONAL DETAILS

The calculations were performed by using density functional theory including the van der Waals interaction (vdW-DFT) as implemented in the SIESTA code.[25] The electron-electron interactions were treated by employing the generalized gradient approximation due to Perdew, Burke, and Ernzerhof.[26] The van der Waals interaction was included within a semiempirical approach, following the Grimme formula.[27] The Kohn-Sham orbitals were described by a linear combination of numerical pseudoatomic orbitals using a split-valence double-ζ basis set including polarization functions. The electron-ion interactions were calculated by using norm-conserving pseudopotentials.[28]

Within our computational approach, there is a lattice mismatch between graphene and the InAs(110) surface. Along the $[1\bar{1}0]$ direction there is a very small mismatch of 0.64% (the experimental mismatch being 0.6%). In order to minimize the strain induced on the graphene sheet, we chose a supercell with six (1×1) units along the [100] direction. This choice leaves a lattice mismatch of 1.38% along the [100] direction. With this consideration, the InAs(110) and the Au-covered InAs(110) surfaces were described by using the slab method, where we considered eight InAs layers and 6×1 surface periodicity. Above the top InAs layer we placed, per surface unit cell, 60 C atoms for the graphene sheet and 34 C atoms for the GNR with monohydrogenated armchair edges. In order to avoid the interaction between a given graphene adsorbed slab and its image (due to the periodic boundary conditions) a vacuum region of 15 Å perpendicular to the slab, i.e., along the [110] direction, was included. We checked the adequacy of our choice of the supercell size following the procedure proposed in Ref. 23.

The self-consistent total charge density was obtained by using a set of three special **k** points to sample the Brillouin zone, while the electronic structure was calculated by using 200 special **k** points. All atomic positions except at the bottom InAs layer were relaxed by using the conjugated gradient scheme, within a force convergence criterion of 20 meV/Å.

III. RESULTS AND COMMENTS

A. Clean InAs(110) surface

The clean cleaved III-V(110) surface retains its primitive (1×1) periodicity, and exhibits a well-established relaxation pattern,[29] as shown in Fig. 1(a). The clean InAs(110) surface exhibits semiconducting character and a few surface states lying within the fundamental band gap. We find an energy band gap of 0.80 eV, larger than the band gap of the InAs bulk phase. This can be attributed to the electronic confinement (perpendicular to the surface) due to the slab method applied to describe the InAs(110)-(1×1) system. Table I presents some structural parameters for the surface, for instance, we find a vertical buckling ($\Delta_{1,\perp}$) of the top layer of 0.80 Å. Those electronic and structural results are in good agreement with previous *ab initio* calculations as well as experimental measurements.[30–34] The upward (downward) relaxation of the As (In) atoms is ruled, in accordance with the so-called electronic counting argument, by an energetic preference for an s^2p^3-like hybridization for the topmost As atoms and threefold-coordinated surface In atoms forming an sp^2-like (planar) hybridization.

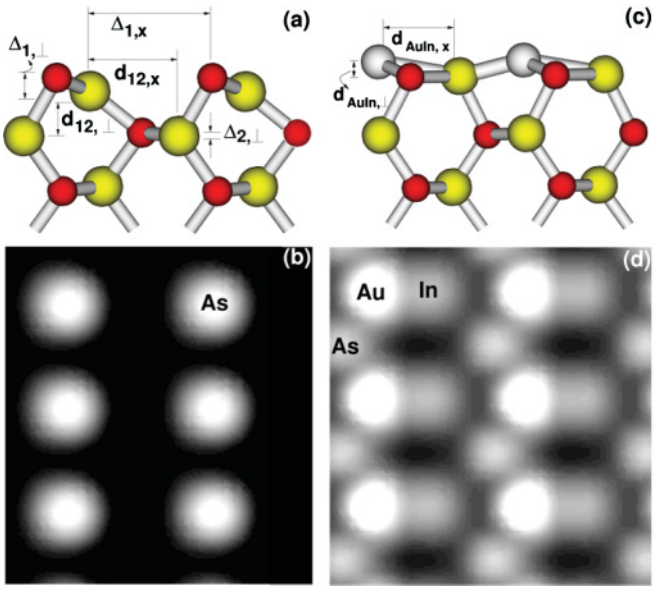

FIG. 1. (Color online) Side view and details of the equilibrium geometry of clean InAs(110) surface (a), and the simulated STM images of the occupied states within $E_F - 2$ eV (b). Equilibrium geometry of the $Au_{(1\ ML)}$/InAs(110) surface (c), and the simulated STM images for $E_F - 2$ eV (d).

Figure 1(b) presents our simulated STM images for the occupied states within an energy interval of 2 eV below the Fermi level ($E_F - 2$ eV), verifying the experimentally observed formation of bright spots on the topmost As atoms.

B. Graphene/InAs(110)

Figure 2(a) presents the structural model for graphene adsorbed on InAs(110). We will refer to this system as G/InAs(110). The graphene adsorption energy (E^{ads}) was calculated by comparing the total energies of the separated components, viz., the graphene sheet and the InAs(110) surface, and the total energy of the (final) graphene adsorbed system:

$$E^{ads} = E[\mathrm{G}] + E[\mathrm{InAs(110)}] - E[\mathrm{G/InAs(110)}] - \delta^{BSSE},$$

where E[G] and E[InAs(110)] represent the total energies of an isolated graphene sheet and the clean InAs(110) surface, respectively, and E[G/InAs(110)] represents the total energy of G/InAs(110). The last term (δ^{BSSE}) was included to correct the basis set superposition error (BSSE).[35] This is necessary, since within our theoretical approach the Kohn-Sham wave functions for the different systems were expanded in different

TABLE I. Structural parameters of the clean InAs(110) surface as indicted in Fig. 1. The atomic relaxations are in angstroms.

	$\Delta_{1,\perp}$	$\Delta_{1,x}$	$\Delta_{2,\perp}$	$d_{12,\perp}$	$d_{12,x}$
Present	0.80	4.88	0.15	1.60	3.57
Theory (Ref. 31)	0.75	4.66	0.13	1.44	3.39
Expt. (Ref. 30)	0.768	4.985	0.140	1.497	3.597

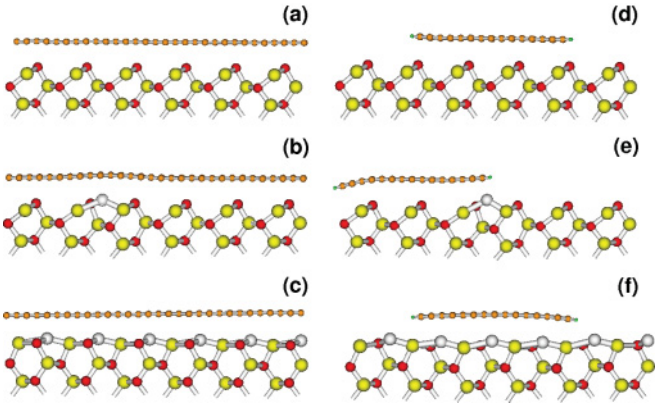

FIG. 2. (Color online) Structural models for graphene adsorbed on the clean InAs(110) surface (a), and Au-covered InAs(110) surfaces, for 1/6 monolayer (ML) (b) and 1 ML (c) of Au adatoms.

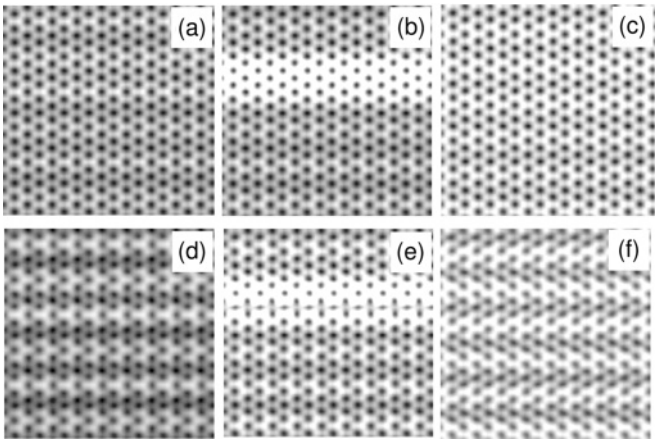

FIG. 3. (Top) Simulated constant-height STM images of the occupied states within $E_F - 2$ eV of G/InAs(110) (a), $G/Au_{(1/6\ ML)}/InAs(110)$ (b), and $G/Au_{(1\ ML)}/InAs(110)$ (c) systems at the equilibrium geometry. (Bottom) Constant-height STM images, within $E_F - 2$ eV, pushing the graphene sheet by 0.3 Å (with respect to the equilibrium geometry) toward the InAs(110) or Au/InAs(110) surface, G/InAs(110) (d), $G/Au_{(1/6\ ML)}/InAs(110)$ (e), and $G/Au_{(1\ ML)}/InAs(110)$ (f) systems.

basis sets of pseudoatomic orbitals. We obtained δ^{BSSE} by following the procedure proposed by Hobbs *et al.*[36]

We find that graphene adsorption on the InAs(110) surface is an exothermic process with E^{ads} of 24 meV/(C atom). Very recently, by using the same approach, we estimated E^{ads} around 50 meV/(C atom) for a graphene sheet adsorbed onto an amorphous SiO_2 surface ($G/a\text{-}SiO_2$),[37] in good agreement with experimental results.[38] There are no chemical bonds between the graphene sheet and the InAs(110) surface, and the sheet lies at a vertical distance (d_z) of 3.20 Å from the topmost As atoms, in agreement with recent experimental STM measurements, $d_z \approx 3$ Å.[22] The adsorbed graphene sheet exhibits a surface (structural) corrugation of ~0.15 Å, while the vertical buckling of the topmost In-As chain, $\Delta_{1,\perp}$, is reduced by only 0.02 Å, to $\Delta_{1,\perp} = 0.78$ Å. We have also considered two other configurations for G/InAs(110), by displacing the graphene sheet along the [100] and [1$\bar{1}$0] directions, where we find the same values of E^{ads} and equilibrium geometry. These results indicate that graphene sheets are weakly attached to the InAs(110) surface, similar to the G/GaAs(110) and $G/a\text{-}SiO_2$ systems.[23,37] Indeed, by turning off the vdW contribution from our total energy calculations, we find $E^{ads} = -3$ meV/(C atom), indicating that the graphene adsorption on the InAs(110) surface is no longer an exothermic process, and the equilibrium distance d_z increases to 3.66 Å.

Figure 3(a) presents our simulated STM image for the occupied states within an energy interval of 2 eV below the calculated Fermi level (E_F). In accordance with previous results for G/GaAs(110),[22] for a vertical distance d_z around 3 Å and an energy interval of $E_F - 2$ eV, the STM simulation depicts the graphene hexagonal lattice with a weak registry of the InAs(110) substrate. However, we notice that there is a net displacement of the electronic charge density on the graphene sheet, giving rise to bright and dark stripes parallel to the [1$\bar{1}$0] direction. The formation of the stripes is due to the relative positions between the hexagonal network of the graphene carbon atoms and the In-As chain underneath. Similar total charge displacement has also been noted for the $G/a\text{-}SiO_2$ systems.[39] The resultant electron-rich and hole-rich regions will act as scattering centers, thus reducing the electronic mobility for graphene in the G/InAs(110) system. Indeed, such a reduction in the electron mobility has been experimentally verified for graphene on $a\text{-}SiO_2$.[9]

Graphene sheets may exhibit a local deformation due to the presence of a scanning tip, which can give rise to different STM pictures.[40] Following the procedure proposed in Ref. 22, in order to mimic the local deformation of the graphene sheet due to its interaction with the scanning tip, we pushed the graphene sheet toward the InAs(110) surface and performed a new set of STM simulations. In this case, for a displacement of 0.3 Å, we found the formation of periodic bright lines as shown in Fig. 3(d). This is due to the presence of the topmost buckled As atoms. Our results thus provide support to the previously advocated transparency results for the G/GaAs(110) system.[22]

It has been suggested that, for physisorbed graphene systems, the presence of empty (occupied) surface electronic states below (above) the Dirac point may promote an electronic charge transfer from (to) the adsorbed graphene sheet, characterizing a noncovalent functionalization of graphene.[23,24] Figures 4(a) and 4(b) present the electronic band structure of the G/InAs(110) system with the graphene sheet lying at $d_z = 5$ and 3.20 Å from the InAs(110) surface, respectively. As expected, far from the surface, the massless metallic bands are maintained [Fig. 4(a)]; whereas, at the equilibrium geometry $d_z = 3.20$ Å [Fig. 4(b)], we find the formation of a small energy gap of 0.01 eV at the Dirac point, indicating that the metallic character of the graphene sheet has been suppressed due to its interaction with the InAs(110) surface. Indeed, a similar (small) band gap opening has been verified for graphene on SiO_2.[41,42] Apart from the narrow gap at the Dirac point, our calculated density of states (DOS) projected on the adsorbed graphene sheet, depicted in Fig. 4(c), indicates that the electronic states of the graphene are only weakly perturbed upon the formation of G/InAs(110). However, through the integration of the projected DOS for the adsorbed and isolated

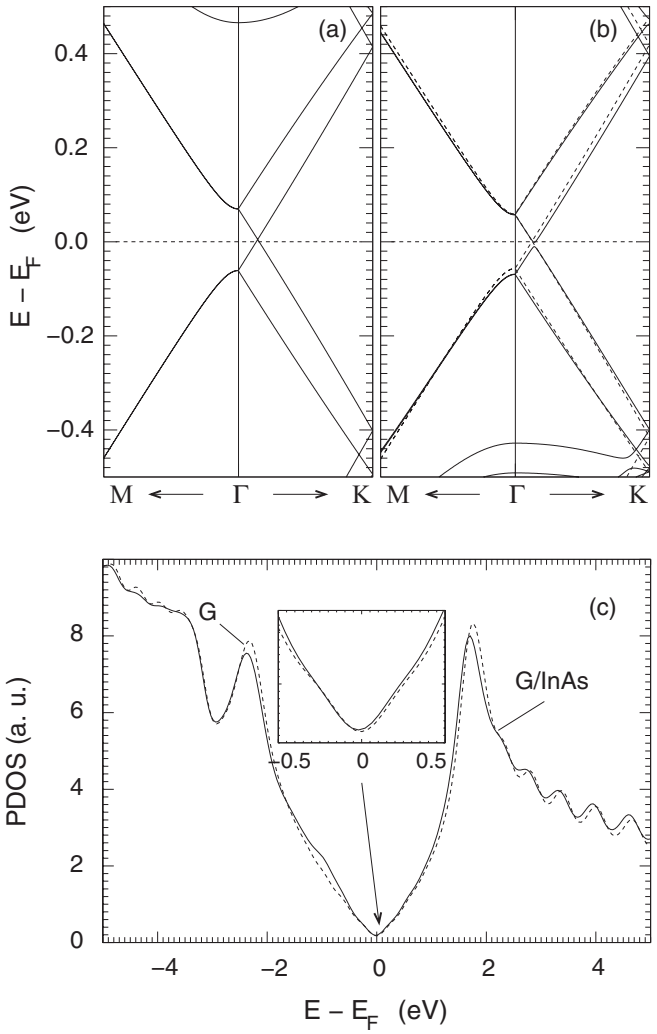

FIG. 4. Electronic band structure of G/InAs(110), for the graphene sheet at 5 Å from the InAs(110) surface (a), and adsorbed (d_z = 3.20 Å) on the InAs(110) surface (b). (c) Partial density of states (PDOS) of G/InAs(110) projected on the graphene sheet. Inset indicates the DOS within an energy interval of $E_F \pm 0.5$ eV. Dashed lines in (b) and (c) represent the band structure and the density of states of an isolated graphene sheet. The DOS was averaged considering a Gaussian width of 0.2 eV.

graphene sheets,[43] we find a small charge transfer of 0.010e/(C atom) from graphene toward the InAs(110) surface.

C. Graphene/Au/InAs(110)

To examine adsorption of graphene on Au-covered InAs(110), Au/InAs(110), we first studied the structural and electronic changes for monolayer (ML) coverages of Au on the InAs(110) surface, a system referred to later as $Au_{(1\ ML)}$/InAs(110). At the equilibrium geometry, the vertical buckling of the top layer on the InAs(110) surface is almost suppressed, with $\Delta_{1,\perp}$ = 0.07 Å. The almost restoration of the bulklike geometry of III-V(110) surfaces upon 1 ML group-V adsorbate coverage is a general feature[29] and has also been verified for a monolayer of Fe adatoms on InAs(110), with $\Delta_{1,\perp}$ = 0.057 Å.[44] For $Au_{(1\ ML)}$/InAs(110), as shown in Fig. 1(c), the Au adatom lies 0.55 Å above the topmost As atom and is threefold coordinated, forming one Au-In and two Au-As bonds of lengths of 2.62 and 2.82 Å, respectively. The Au adatoms add electronic states near the Fermi level, as we can observe in the simulated STM images presented in Fig. 1(d) within $E_F - 2$ eV.

TABLE II. Adsorption energies and equilibrium distances of the graphene sheet and graphene nanoribbon adsorbed on InAs(110), $Au_{(1/6\ ML)}$/InAs(110), and $Au_{(1\ ML)}$/InAs(110).

Structure	E^{ads} [meV/(C atom)]	d_z (Å)
G/InAs(110)	24	3.20
G/$Au_{(1/6\ ML)}$/InAs(110)	28	3.20
G/$Au_{(1\ ML)}$/InAs(110)	22	3.08
GNR/InAs(110)	36	3.24
GNR/$Au_{(1/6\ ML)}$/InAs(110)	45	2.47
GNR/$Au_{(1\ ML)}$/InAs(110)	46	2.56

The presence of Au adatoms changes the adsorption energy slightly when compared with that for G/InAs(110). We calculated E^{ads} = 22 meV/(C atom). It is worth noting that this result is close to the adsorption energy of graphene on the Au(111) surface, 30 meV/(C atom), obtained from a DFT local spin density approximation calculation.[24] As in the G/InAs(110) system, there are no chemical bonds between the graphene sheet and the $Au_{(1\ ML)}$/InAs(110) surface. At the equilibrium geometry, Fig. 2(c), we find $d_z \approx 3.08$ Å (see Table II). The STM simulation presented in Fig. 3(c) shows that the hexagonal pattern of carbon atoms becomes brighter in comparison with the STM image of G/InAs(110). This is due to an increase in the density of states around E_F because of the presence of Au adatoms.

The adsorption energy of graphene on (1/6 ML)-covered Au/InAs(110), $Au_{(1/6\ ML)}$/InAs(110), is 28 meV/(C atom), almost the same as for 1 ML of Au. The vertical separation between graphene and Au is 3.20 Å, slightly larger than that for 1 ML coverage of Au. The C atoms above the Au adatoms move upward by 0.33 Å with respect to the planar region of the adsorbed graphene sheet, Fig. 2(b). Such a vertical displacement produces the formation of a bright line above the Au adatoms in the simulated STM image along the [1$\bar{1}$0] direction, as seen in Fig. 3(b). However, we find that the hexagonal pattern of carbon atoms is dimmer in comparison with G/$Au_{(1\ ML)}$/InAs(110), due to relatively less increase in the density of states around E_F.

Similar to what we have done for G/InAs(110), the local deformation of the graphene sheet, on the STM images, was examined by pushing the graphene sheet by 0.3 Å toward the Au/InAs(110) surface and keeping the same energy interval, $E_F - 2$ eV. In this case, we verified the presence of Au atoms below the graphene sheet, as seen in Figs. 3(e) and 3(f). That is, the graphene transparency effect remains evident in Fig. 3(f). Here, unlike in Fig. 3(d), the formation of periodic bright lines is due to the Au adatoms instead of As atoms.

The Fermi levels of the (isolated) $Au_{(1/6\ ML)}$/InAs(110) and $Au_{(1\ ML)}$/InAs(110) metallic surfaces lie below the calculated work function of an isolated graphene sheet (W_G = 4.22 eV) by 0.38 and 0.30 eV, respectively. Thus, if the electronic band structures of the isolated systems do not change upon

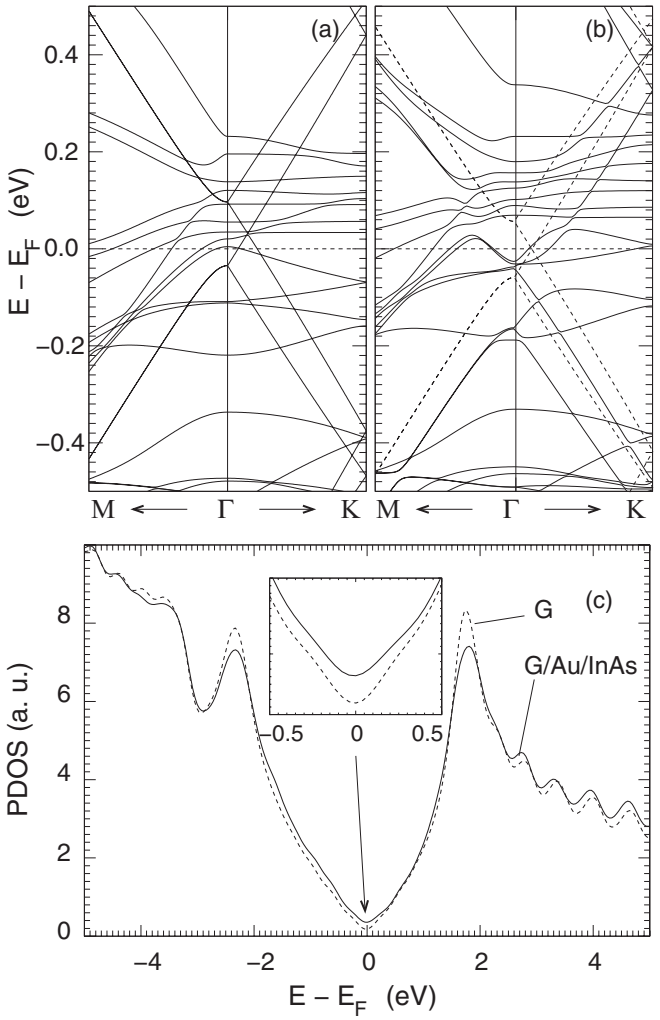

FIG. 5. Electronic band structure of $G/Au_{(1\ ML)}/InAs(110)$, for the graphene sheet at 5 Å from the $Au_{(1\ ML)}/InAs(110)$ surface (a), and adsorbed ($d_z = 3.08$ Å) on the $Au_{(1\ ML)}/InAs(110)$ (b). (c) Density of states (DOS) of $G/Au_{(1\ ML)}/InAs(110)$ projected on the graphene sheet. The inset indicates the DOS within an energy interval of $E_F \pm 0.5$ eV. Dashed lines in (b) and (c) represent the band structure and the density of states of an isolated graphene sheet. The DOS was averaged considering a Gaussian width of 0.2 eV.

the formation of the G/Au/InAs(110) system, we can infer an electronic charge transfer from the adsorbed graphene sheet to the Au/InAs(110) surface, i.e., a *p*-type doping of the adsorbed graphene. It is interesting to note that a *p*-type doping for graphene adsorbed on the Au(111) surface was also suggested in a recent theoretical investigation by Khomyakov *et al.*[24] However, these authors pointed out that an electronic charge transfer between the adsorbed graphene and the metallic substrate cannot be inferred just based on the relative positions of W_G and E_F of the metallic surface, considering isolated systems. The interaction between the adsorbed graphene sheet and the surface plays an important role. Figures 5(a) and 5(b) present the electronic band structure of $G/Au_{(1\ ML)}/InAs(110)$ calculated for $d_z = 5$ Å (far from the surface) and $d_z = 3.08$ Å (equilibrium geometry), respectively. In Fig. 5(a) we verify the linear metallic bands at the Dirac point, namely, the electronic band structure of the graphene has been mantained, but embedded in the metallic bands of the $Au_{(1\ ML)}/InAs(110)$ surface. In this case, there is a net charge transfer at the $G\text{-}Au_{(1\ ML)}/InAs(110)$ interface, the graphene sheet presents a *p*-type doping, and the Fermi level equilibrates at ∼0.03 eV below the Dirac point. Meanwhile, at the equilibrium geometry [$d_z = 3.08$ Å, Fig. 5(b)] we verify that electronic interactions take place at the $G\text{-}Au_{(1\ ML)}/InAs(110)$ interface, and the linear metallic bands of the graphene sheet are suppressed within an energy interval of $E_F \pm 0.1$ eV. Through the calculation of the DOS projected on the adsorbed graphene sheet [Fig. 5(c)] we find that the electronic states of the graphene sheet are weakly perturbed upon its interaction with the surface. In this case, there is a net electronic charge transfer of $0.012e$/(C atom) from the adsorbed graphene sheet toward $Au_{(1\ ML)}/InAs(110)$.[43] Similar results were obtained for $G/Au_{(1/6\ ML)}/InAs(110)$.

To further understand the above statements, it is important to realize that there is a net electronic charge displacement $\Delta\rho(z)$ at the G-Au/InAs(110) interface (Fig. 6), giving rise to an electronic dipole perpendicular to the Au/InAs(110) surface. We express $\Delta\rho(z)$ as

$$\Delta\rho(z) = \frac{1}{A_{xy}} \int \Delta\rho(\mathbf{r}) dx\, dy,$$

where A_{xy} is the surface unit cell and $\Delta\rho(\mathbf{r})$ is

$$\Delta\rho(\mathbf{r}) = \rho_{G/Au/InAs(110)}(\mathbf{r}) - \rho_G(\mathbf{r}) - \rho_{Au/InAs(110)}(\mathbf{r}),$$

with ρ_G, $\rho_{Au/InAs(110)}$, and $\rho_{G/Au/InAs(110)}$ representing the total charge densities of the isolated graphene sheet, the Au/InAs(110) surface, and the G/Au/InAs(110) adsorbed system, respectively. For the $G/Au_{(1ML)}/InAs(110)$ system [left panel in Fig. 6] we find $\Delta\rho(z) < 0$ at around 1 Å below the adsorbed graphene sheet, while there is an increase in the electronic charge density $\Delta\rho(z) > 0$ at 2 Å above the $Au_{(1\ ML)}/InAs(110)$ surface. A similar $\Delta\rho(z)$ result has been verified for $G/Au_{(1/6\ ML)}/InAs(110)$ system: there is a decrease in the total charge density at 1.5 Å below the adsorbed graphene sheet, while $\Delta\rho(z) > 0$ occurs near the

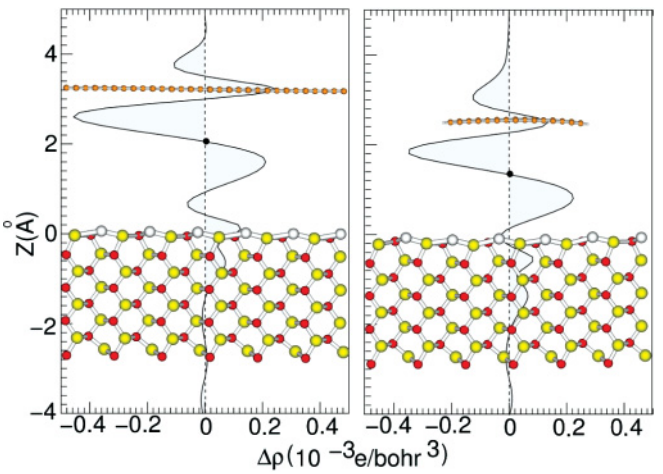

FIG. 6. (Color online) Planar average of the electronic charge density transfer, along the [110] direction, of $G/Au_{(1\ ML)}/InAs(110)$ (left panel) and $GNR/Au_{(1\ ML)}/InAs(110)$ (right panel) systems.

Au/InAs(110) surface region. In addition, it is noticeable that, for both systems, $\Delta\rho(z)$ goes to zero a few layers below the Au/InAs(110) surface. That is, the electronic perturbations as well as the formation of an electric dipole upon graphene adsorption are mostly localized at the G-Au/InAs(110) interface region. Such a distribution of $\Delta\rho(z)$ gives rise to an electric dipole at the G-Au/InAs(110) interface. The development of the dipole reduces the electronic charge transfer from the graphene toward the Au/InAs(110) surface, thus hindering doping of the graphene sheet.

D. GNR/InAs(110) and GNR/Au/InAs(110)

We further examined adsorption of an armchair graphene nanoribbon on the InAs(110) and Au/InAs(110) surfaces. Armchair GNRs with (mono)hydrogenated edge C atoms present a semiconducting character, with reduction in the energy band gap with increase in the width of the ribbon. We considered a GNR with a width of 17 Å, which corresponds to seven hexagonal carbon rings aligned along the [100] direction with respect to the InAs(110) surface. Our calculated adsorption energies indicate that the nanoribbon is more strongly attached to the InAs(110) and Au/InAs(110) surfaces than is the graphene sheet. The calculated adsorption energies and the equilibrium distances for the energetically most stable configurations, depicted in Figs. 2(d)–2(f), are summarized in Table II. As for G/InAs(110), there is no chemical bonding between the nanoribbon and the InAs(110) surface, and the ribbon keeps it planar structure, as shown in Fig. 2(d). In contrast, a weak chemical interaction takes place between Au/InAs(110) and the edge sites for both 1/6 ML and 1 ML coverages of Au. As shown in Figs. 2(e) and 2(f), the adsorbed GNR assumes a bent geometry, and lies at an average height d_z of around 2.5 Å above the surface.

We find an energy band gap of 0.53 eV for the isolated GNR. The semiconducting character of the adsorbed GNR has been maintained. Figure 7(a) presents the electronic band structure of GNR/InAs(110), where the highest occupied and lowest unoccupied states are localized on the carbon atoms of the adsorbed GNR. Through the calculation of the DOS projected onto the GNR [Fig. 7(c)], we verify that its electronic states are weakly perturbed, with small electronic charge transfer from the GNR to the InAs(110) surface, $0.096e$/(C atom).[43] On the other hand, the GNR/$Au_{(1\ ML)}$/InAs(110) system is metallic, Fig. 7(b), where the partially occupied states are mostly ruled by the Au adatoms of the surface. In this case, as in the G/Au/InAs(110) system, by comparing the Fermi energy of the Au/InAs(110) surface and the ionization potential of the GNR, we may infer an electronic charge transfer from the GNR to the empty states of the Au/InAs(110) surface. We calculate an ionization potential of 4.21 eV for an isolated armchair GNR, which is 0.31 eV above the Fermi level of the isolated $Au_{(1\ ML)}$/InAs(110) surface, thus suggesting the formation of p-type doped GNR adsorbed on $Au_{(1\ ML)}$/InAs(110). Our calculated DOS projected onto the GNR, Fig. 7(d), indicates that there is a (small) electronic charge transfer of $0.081e$/(C atom) from the nanoribbon to the $Au_{(1\ ML)}$/InAs(110) surface. There is a net charge density displacement $\Delta\rho(z)$ at the GNR-InAs(110) and GNR-Au/InAs(110) interfaces, giving rise to an electric dipole along the [110] direction [perpendicular to the InAs(110) surface]. The right hand panel in Fig. 6 presents $\Delta\rho(z)$ for the GNR/$Au_{(1\ ML)}$/InAs(110) system. As in the G/Au/InAs(110) system, the electrons from the GNR will face an additional potential in moving from the GNR toward the InAs(110) or Au/InAs(110) surface, thus inhibiting the doping process.

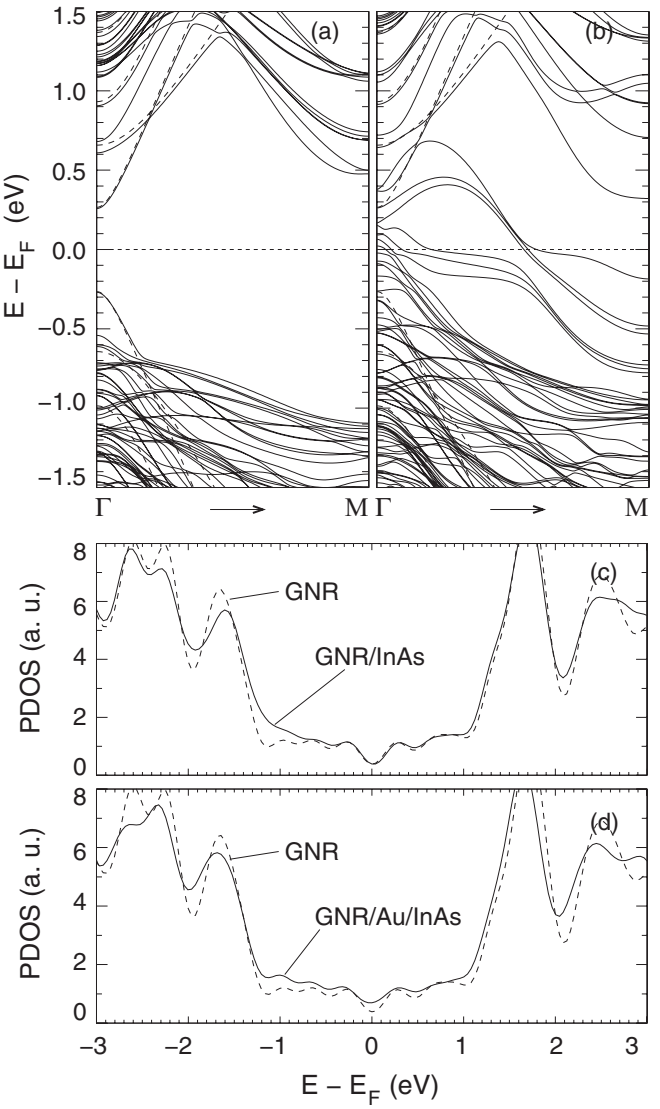

FIG. 7. Electronic band structures of GNR/InAs(110) (a) and the GNR/Au_{1ML}/InAs(110) (b) systems. Densities of states of GNR/InAs(110) (c) and GNR/Au/InAs(110) (d), projected on the adsorbed GNR. Dashed lines represent the band structure and density of states of an isolated GNR. The DOS was averaged considering a Gaussian width of 0.2 eV.

IV. SUMMARY

In summary, we find that the monolayer graphene sheet is weakly attached to the InAs(110) and Au/InAs(110) surfaces. The formation of stable G/InAs(110) and G/Au/InAs(110) systems is ruled by vdW interactions, with adsorption energies of around 25 meV/(C atom). Although there are no chemical bonds between the graphene sheet and the substrates, there is a small charge transfer from the graphene sheet toward

the adsorption surfaces. However, the resulting *p*-type doping of the adsorbed graphene sheet is somewhat inhibited by the formation of an electric dipole at the graphene-surface interface. Graphene nanoribbons are more strongly attached to InAs(110) and Au/InAs(110) surfaces, in comparison with their G/InAs(110) and G/Au/InAs(110) counterparts. The calculated adsorption energies of the 17-Å-wide armchair graphene nanoribbon on these surfaces are ∼40 meV/(C atom). There is a weak chemical interaction between the edge sites of the GNR and Au/InAs(110). Our electronic structure results suggest that there is a small net charge transfer from the nanoribbon to the InAs(110) and Au/InAs(110) surfaces, and the formation of an electric dipole at the GNR–InAs(110) and GNR–Au/InAs(110) interfaces.

ACKNOWLEDGMENTS

D.P.A. and R.H.M. acknowledge the Brazilian agencies CNPq, CAPES, and FAPEMIG for financial support and the CENAPAD-Campinas for the computer facilities.

[1] S. Iijima, Nature (London) **354**, 2148 (1991).
[2] A. K. Geim and K. S. Novoselov, Nat. Mater. **6**, 183 (2007).
[3] H. Lee, Y.-W. Son, N. Park, S. Han, and J. Yu, Phys. Rev. B **72**, 174431 (2005).
[4] Y.-W. Son, M. L. Cohen, and S. G. Louie, Phys. Rev. Lett. **97**, 216803 (2006).
[5] K. A. Ritter and J. W. Lyding, Nat. Mater. **8**, 235 (2009).
[6] A. H. C. Neto, F. Guinea, N. M. R. Peres, K. S. Novoselov, and A. K. Geim, Rev. Mod. Phys. **81**, 109 (2009).
[7] X. Du, I. Skachko, F. Duerr, A. Luican, and E. Y. Andrei, Nature (London) **462**, 192 (2009).
[8] Y. Wu, Yu.-m. Lin, A. A. Bol, K. A. Jenkins, F. Xia, D. B. Farmer, Y. Zhu, and P. Avouris, Nature (London) **472**, 74 (2011).
[9] M. C. Lemme, T. J. Echtermeyer, M. Bauss, and H. Kurz, IEEE Electron Device Lett. **28**, 282 (2007).
[10] J. S. Soares *et al*., Nano Lett. **10**, 5043 (2010).
[11] W. Orellana, R. H. Miwa, and A. Fazzio, Phys. Rev. Lett. **91**, 166802 (2003).
[12] R. H. Miwa, W. Orellana, and A. Fazzio, Appl. Phys. Lett. **86**, 213111 (2005).
[13] S. Barraza-Lopez, P. M. Albrecht, N. A. Romero, and K. Hess, J. Appl. Phys. **100**, 124304 (2006).
[14] P. M. Albrecht, S. Barraza-Lopez, and J. W. Lyding, Nanotechnology **18**, 095204 (2007).
[15] S. Barraza-Lopez, P. M. Albrecht, and J. W. Lyding, Phys. Rev. B **80**, 045415 (2009).
[16] S. Berber and A. Oshiyama, Phys. Rev. Lett. **96**, 105505 (2006).
[17] Z. Zhang, C. Chen, X. C. Zeng, and W. Guo, Phys. Rev. B **81**, 155428 (2010).
[18] L. B. Ruppalt and J. W. Lyding, Nanotechnology **18**, 215202 (2007).
[19] H. Romero, N. Shen, P. Joshi, H. R. Gutierrez, S. A. Tadigadapa, J. O. Sofo, and P. C. Eklund, ACS Nano **2**, 2037 (2008).
[20] S. Berciaud, S. Ryu, L. E. Brus, and T. F. Heiz, Nano Lett. **9**, 346 (2009).
[21] S. M. Song and B. J. Cho, Nanotechnology **21**, 335706 (2010).
[22] K. T. He, J. C. Koepke, S. Barraza-Lopez, and J. W. Lyding, Nano Lett. **10**, 3446 (2010).
[23] T. A. G. Eberlein, R. Jones, J. P. Goss, and P. R. Briddon, Phys. Rev. B **78**, 045403 (2008).
[24] P. A. Khomyakov, G. Giovannetti, P. C. Rusu, G. Brocks, J. van den Brink, and P. J. Kelly, Phys. Rev. B **79**, 195425 (2009).
[25] J. M. Soler, E. Artacho, J. D. Gale, A. García, J. Junquera, P. Ordejón, and D. Sánchez-Portal, J. Phys.: Condens. Matter **14**, 2745 (2002).
[26] J. P. Perdew, K. Burke, and M. Ernzerhof, Phys. Rev. Lett. **77**, 3865 (1996).
[27] S. Grimme, J. Comput. Chem. **27**, 1787 (2006).
[28] N. Troullier and J. L. Martins, Phys. Rev. B **43**, 1993 (1991).
[29] G. P. Srivastava, Rep. Prog. Phys. **60**, 561 (1997).
[30] C. B. Duke, A. Paton, A. Kahn, and C. R. Bonapace, Phys. Rev. B **27**, 6189 (1983).
[31] J. L. A. Alves, J. Hebenstreit, and M. Scheffler, Phys. Rev. B **44**, 6188 (1991).
[32] J. Klijn, L. Sacharow, C. Meyer, S. Blügel, M. Morgenstern, and R. Wiesendanger, Phys. Rev. B **68**, 205327 (2003).
[33] J. R. Weber, A. Janotti, and C. G. Van de Walle, Appl. Phys. Lett. **97**, 192106 (2010).
[34] M. G. Betti, G. Bertoni, V. Corradini, V. De Renzi, and C. Mariani, Surf. Sci. **454-456**, 539 (2000).
[35] S. F. Boys and F. Bernardi, Mol. Phys. **19**, 553 (1970).
[36] C. Hobbs, K. Kantorovich, and J. D. Gale, Surf. Sci. **591**, 45 (2005).
[37] R. H. Miwa, T. M. Schmidt, W. L. Scopel, and A. Fazzio, Appl. Phys. Lett. **99**, 163108 (2011).
[38] M. Ishigami, J. H. Chen, W. G. Cullen, M. S. Fuhrer, and E. D. Williams, Nano Lett. **7**, 1643 (2007).
[39] J. Martin, N. Akerman, G. Ulbricht, T. Lohmann, J. H. Smet, and K. Von Klitzing, Nat. Phys. **4**, 144 (2008).
[40] T. Mashoff, M. Pratzer, V. Geringer, T. J. Echtermeyer, M. C. Lemme, M. Liebmann, and M. Morgenstern, Nano Lett. **10**, 461 (2010).
[41] Y. J. Kang, J. Kang, and K. J. Chang, Phys. Rev. B **78**, 115404 (2008).
[42] N. T. Cuong, M. Otani, and S. Okada, Phys. Rev. Lett. **106**, 106801 (2011).
[43] The net electronic charge transfers were calculated by comparing the integrated (occupied) densities of states, projected onto the carbon atoms of the isolated and adsorbed graphene sheet or graphene nanoribbons.
[44] L. Sacharow, M. Morgenstern, G. Bihlmayer, and S. Blügel, Phys. Rev. B **69**, 085317 (2004).